



## Overview in Technical Synthesis and Applications of $Zr_2AC$ (A= In, Sn, Pb, Al, S and Se) MAX phases: a brief review

Dumooa R. Hussein , Khalid K. Abbas\* , Ahmed M.H. Abdulkadhim Al-Ghaban 

Materials Engineering Dept., University of Technology-Iraq, Alsina'a street, 10066 Baghdad, Iraq.

\*Corresponding author Email: [mae.19.05@grad.uotechnology.edu.iq](mailto:mae.19.05@grad.uotechnology.edu.iq)

### HIGHLIGHTS

- The bulk  $Zr_2AC$  ceramic MAX phase can be produced by hot isostatic pressing sintering, hot press sintering, and pressureless sintering.
- At the higher temperatures, the MAX phase decomposes into MC and intermetallic compounds.
- The most interesting  $Zr_2AC$  MAX phase in nuclear applications.
- Providing insight, the potential research prospects for this  $Zr_2AC$  MAX phases in numerous fields.

### ARTICLE INFO

**Handling editor:** Mustafa H. Al-Furaiji

**Keywords:**

$Zr_2AC$  ; MAX phase ; Hot isostatic pressing  
Hot press sintering ; Pressureless ; Nuclear

### ABSTRACT

$Zr_2AC$  MAX phases are ternary carbide family with layered structures combining of the outstanding characteristics of metals and ceramics. This review study provides an overview of  $Zr_2AC$  MAX phase formation mechanisms, applications, and the correlation between  $Zr_2AC$  MAX phase formation mechanisms and performance in applications such solar coatings, oxidation resistance, high temperature applications, and nuclear applications.  $Zr_2InC$  MAX phase has low friction and wear materials that can be used for variety applications for significant technology such as electrical spinning connections and rotating bearings. More examples, the  $Zr_2SnC$  MAX phase uses for self-healing of cracks and oxidation resistance. The  $Zr_2PbC$  MAX phases are elastic and electrically anisotropic in nature and appropriate for high temperature applications, optoelectronic devices, and coating materials. Studying the optical characteristics of the  $Zr_2SeC$  has shown its potential for application as a shielding material in order to decrease the heating of solar. The  $Zr_2SC$  is suitable for use in high-temperature technologies, such as thermal barrier coating material TBC. The  $Zr_2AlC$  phase is the most attractive among all non-synthesizable ternary MAX phases, particularly for the nuclear industry. There are a lot of challenges during fabrication of the MAX phase, including synthesis temperature, the MAX phase purity, and the secondary phase (impurities). In harsh external conditions, the defect density has a substantial impact on the MAX phase's stability and thus, the methods of defect formation and migration have a considerable impact on the phases' radiation resistance and self-healing capabilities.

## 1. Introduction

Over the history of MAX phases, the MAX phases have been widely accepted by researchers because of their distinctive features and its application. In the early 1960s, almost 100 new MAX phases of carbides and nitrides were discovered by Jeitschko and Nowotny [1,2]. Nowotny's group in Vienna discovered the MAX phases for the first time in 1960. The experimental synthesis of compounds of the 211 phases (for example,  $Ti_2AlC$ , termed to then as "H-phases") and  $Ti_3SiC_2$  and  $Ti_3GeC_2$  of the 312 phases were successfully done. As Nowotny's study in the 1980s, Dr. Schuster discovered the  $Ti_3AlC_2$  compound. Interestingly, there until 1996 and 1997, there was a shortage of attention in this phase [3, 4]. Barsoum and El-Raghy subsequently published their study regarding ternary carbides, which have a number of outstanding features including good electrical and thermal conductivity, machinability, and high resistance to oxidation and thermal shock [5]. After the discovery of  $Ti_4AlN_3$  with  $n = 3$  or 413 phases in 1999, it was addressed as  $M_{n+1}AX_n$ , also known as the MAX phase short form. In addition, researchers at Linköping University in Sweden found the quaternary 312 MAX phase in 2014 [4].

The  $M_{n+1}AX_n$ , known as 211, 312, 413 MAX phases for  $n = 1, 2, 3$ , respectively [6, 7]. Numerous research suggested that replacement on the M, A, or X site in the MAX phase  $M_{n+1}AX_n$  that can enhance their mechanical, chemical, and physical properties. Therefore, by substituting on M, A, or X sites, MAX phase solid solutions hold the potential to improve the characteristics of this class of materials for many prospective applications [4]. Varying number of solid-solution MAX compounds have been created and described in the intervening years. All known MAX phases as of the end of 2014 were made of single M element or arbitrary solid solution quaternaries with the M, A, and / or X sites. The first chemically ordered

quaternary 312 MAX phase was reported in 2014. Shortly after, the University of Poitiers in France proved the existence of more ordered phases, which included 413 composition of MAX phases and were referred to as o-MAX for out-of-plane order. In-plane ordering, also known as the i-MAX phase, was found in 2017 at Linköping University in Sweden [8]. There are now roughly 80 compounds (from the MAX phase) that have been synthesized, and there are theoretically 155 known MAX phases ( $M_{n+1}AX_n$ ,  $n = 1-4$ ) out of a possible 665 feasible MAX phases. However, both theoretical and experimental reports are being carried much more frequently. Research in the MAX phase nanolaminates has become a significant field of research in the world of materials science. Scientific communities are always interested in the development of new MAX phase solid solutions since it is one of the most effective ways to change the properties of already-existing MAX phase materials, opening up new fields of investigation and expanding their range of applications. It has been claimed that the solid solutions have improved a number of significant characteristics, including oxidation, fracture toughness, strength, and self-healing properties [9].

In this direction, recently the scientific community has been showing a substantial interest in MAX phase solid solutions to enhance the physical properties by ( $M'_xM''_{1-x}$ ) $_n$  $AX_n$ ,  $M_{n+1}(A'_xA''_{x-1})X_n$  or C, N and B in the case of X-site solid solutions [8]. For example, inclusion of  $M_n$  element on the M-site, this allows to obtain an opportunity to synthesize metallic-based nanolamellar materials, especially with the desired electronic and magnetic properties [4]. The MAX-phase family, which includes the materials  $Cr_2GaC$ , Mn-doped  $Cr_2GaC$ ,  $Cr_2GaN$   $Cr_2GeC$ ,  $Cr_2AlC$ , (V, Mn) $_3GaC_2$ , and (Mo, Mn) $_2GaC$ , can also exhibit permanent magnetic activity [10]. Recently, the C/N atom was replaced with a boron atom by Aysenur Gencer et al. and Gokhan Surucu et al. The high neutron cross-section of boron makes these MAX phase boride ceramics, which are new materials, stable and effective in control rods in nuclear reactors [11]. The MAX phases are also excellent optical and electrical conductors' properties. Furthermore, from the MAX phases, it can be produced the MXene structures in two dimensions [12, 13], which are used in sodium ion and Lithium ion batteries and super capacitors [13,14]. The MXene are hydrophilic with excellent conductivity and are being important for a high applications host [15].

Material, such as metals, had high electrical and thermal conductivity with excellent machinability. Similar to ceramics, the MAX phase was also resistant to oxidation and thermal shock. They found that phases had a distinct fundamental structure, giving them equivalent metal characteristics [16–18].

The  $M_{n+1}AX_n$  (or simply MAX) phases are a family of intrinsically nanolaminates ternary carbides, nitrides and borides with over 80 members. In the notation of  $M_{n+1}AX_n$ , M refers to the early and late transition metals (Sc, Ti, Zr, Hf, V, Nb, Ta, Cr, Mn, and Mo) from groups 3–6, A comes from the old American nomenclature for 12–16 groups elements (Cd, Al, Ga, In, Tl, Si, Ge, Sn, Pb, P, As, and S) in the periodic table and X is carbon or nitrogen or boron. The integer  $n$  generally varies from 1 to 3 and its highest value so far has been found experimentally 6. Structurally, the MAX phases are composed of  $M_{n+1}X_n$  ceramic sheets sandwiched in between metallic A-layers of one-atom-thick [5–7].

The term " $M_{n+1}AX_n$ " was recently reduced to "MAX", with well-known MAX phases. The near close-packed M layers are interleaved by A element layers and atoms of X fill the octahedral positions between the M early transition metal. The edge-sharing  $M_6X$  octahedrals are identical with those found in rock salt. Based on the value of  $n$ , MAX phases have been divided into the following groups [19–21]:  $M_2AX$  (211 phase)[19],  $M_3AX_2$  (312 phase)[20],  $M_4AX_3$  (413 phase)[21],  $M_5AX_4$  (514 phase)[22],  $M_6AX_5$  (615 phase),  $M_7AX_6$  (716 phase), hybrid MAX phases 523 phase (211 phase + 312 phase) and 725 phase (413 phase + 514 phase)[23], and  $M_2AB_2$ (212 phase) and  $M_3AB_4$  (314phase) boride MAX phases[12], [24– 26]. Moreover, there is also another class of MAX phase such as 221 phase[27]. The number of M layers between the A layers vary significantly between the three structures as illustrated in Figure 1.1: there are two in the 211 phase, three in the 312 phase, and four in the 413 phase. By similarity, the rest of the 514 phase, 615 phase, and 716 phase can be deduced. This layering structure results in some outstanding MAX phases characteristics [28].

M-X bonds are mixed metallic-covalent, whereas M-A bonds are poor resulting an extremely powerful material [29]. Thermal shock and oxidation resistance are regarded to be strong in the MAX phases [2]. They are relatively soft, have great strength at high temperatures, and may be machined without oil using standard fast speed tools.

The density of states at the Fermi level is large and dominated by the d-d orbitals of the M elements, which explains why they are all metallic-like conductors (with resistivity ranging from 0.07 to 2  $\mu\Omega.m$ ). Their conductivities in some situations exceed those of their pure M element. They all deform when compressed due to ripplation nucleation, which then causes kink bands to develop clearly. In addition, they are relatively soft (Vickers hardness values vary from 1.4 to 8 GPa), damage-resistant, and plastic at high temperatures. Due to their electrical conductivity, which ranges from 12 to 60  $W K^{-1} m^{-1}$  at ambient temperature, they are all largely thermally conductive. They demonstrate, in some situations, unusual thermal-shock behavior, which is when the post-quenched strengths of the material are higher than their pristine counterparts. They are relatively thermal-shock resistant [8].

MAX phase perform excellently in a variety of technological and industrial application, including machinable refractories, ductile, high – temperature heating components, electrical connections for coatings, nuclear application, superconductivity, fuel cells, nuclear industries, and spintronics, which have recently demonstrated promise as thermal barrier coatings (TBC) [11].

The structural, mechanical, electronic, electrical, optical, and bonding properties of the 211 MAX phases have been determined by a combination of theoretical calculations with laboratory experiments. There are currently around 50  $M_2AX$  phases discovered among them. Nevertheless, all possible combinations cannot obtain MAX phases as stable thermodynamically. Additionally, substitutions on the "M," "A," and/or "X" sites can lead to essentially an infinite number of solid solutions [12], [30–33]. The compositions of solid solutions that are thermodynamically stable have not been established yet, and the maximum solubility for any system is still unknown due to the enormous number of possible permutations. Some substances have a low solubility, whereas others have a wide range (0 - 1.11). Contrary to popular belief, even when end-member MAX phases are instability, solid solutions can be produced [8, 34, 35]. Preparation of two M elements onto the

crystal's 2 separate M Wyckoff sites, along with their enhanced ordering stability, are regarded with contributing to the solutions' stability [35]. The synthesis of novel phases and solid solutions has dominated research on MAX phases since 2000. For any researchers looking for a description of the MAX phases, Barsoum produced an excellent book in 2013 titled "MAX phases: Properties of Ternary Carbides and Nitrides" [36]. This book carefully collects a lot of information [37]. In this review, different techniques to synthesize the most often reported ternary MAX phases with A (element from IIIA group or IVA group as show in Figure 1 and formal  $Zr_2AC$  are summarized. The various synthesis protocols are described for each substance.

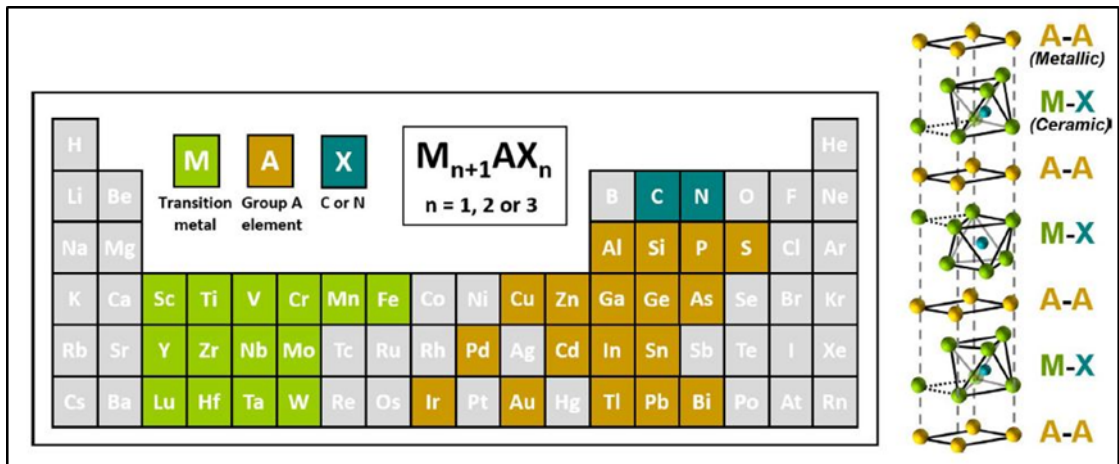
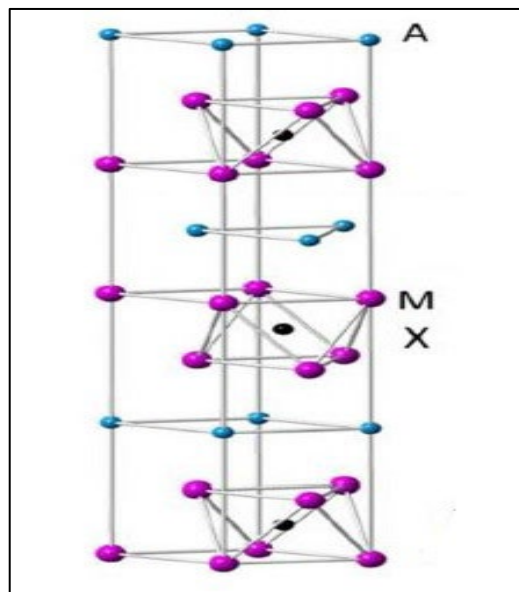


Figure 1: Periodic Table Elements of the unit cell for  $n = 1$  that found in MAX phases [37]

## 2. Technical Methods to Synthesize $Zr_2AC$ MAX Phases

$211$  ( $M_2AX$ ) MAX-phase crystals with Wyckoff positions M (4f), A (2d), and X (2a) and hexagonal symmetry in the space group  $P6_3/mmc$  are shown in Scheme 1. They possess the majority of the potentials requirement today in the field of current technologies, and unique distinctive qualities of metal and ceramic. The key to utilize their potential engineering is to comprehend their stoichiometry and distinctive crystal structure, thus it's crucial to properly identify their unique basic characteristics [38].

Zr-based materials are considering to the nuclear industry due to atoms of Zr contain a tiny cross section for thermal neutron. In addition to this cost consideration, the fuel cladding materials of next generation (Gen-III+) light water reactors ( $LWR_s$ ) must withstand an extreme operating conditions, including mechanical, thermal, significant neutron irradiation, and extremely oxidative or corrosive surroundings. Due to remarkable qualities of MAX phases, whether in bulk state or as coatings, MAX phases consider as suitable materials for cladding of fuel applications. The majority of Zr-based MAX phases with In, Pb, S, Sn, or Tl as the A element have been reported. These phases have crystallographic similarities to the normal MAX phases, but due to their greater hardness, they are harder to machine with conventional equipment [39]. The majority of engineering materials are utilized in bulk. High purity MAX phase are required for nuclear fuel cladding applications because they have good mechanical qualities, coolant compatibility (anti-corrosion, anti-oxidation), and radiation resistance [40]. Different processing techniques are used to fabricate bulk MAX phases [28]. These techniques are described in the following part. Table 1 Shows the comparison between the MAX phase synthesis processes.



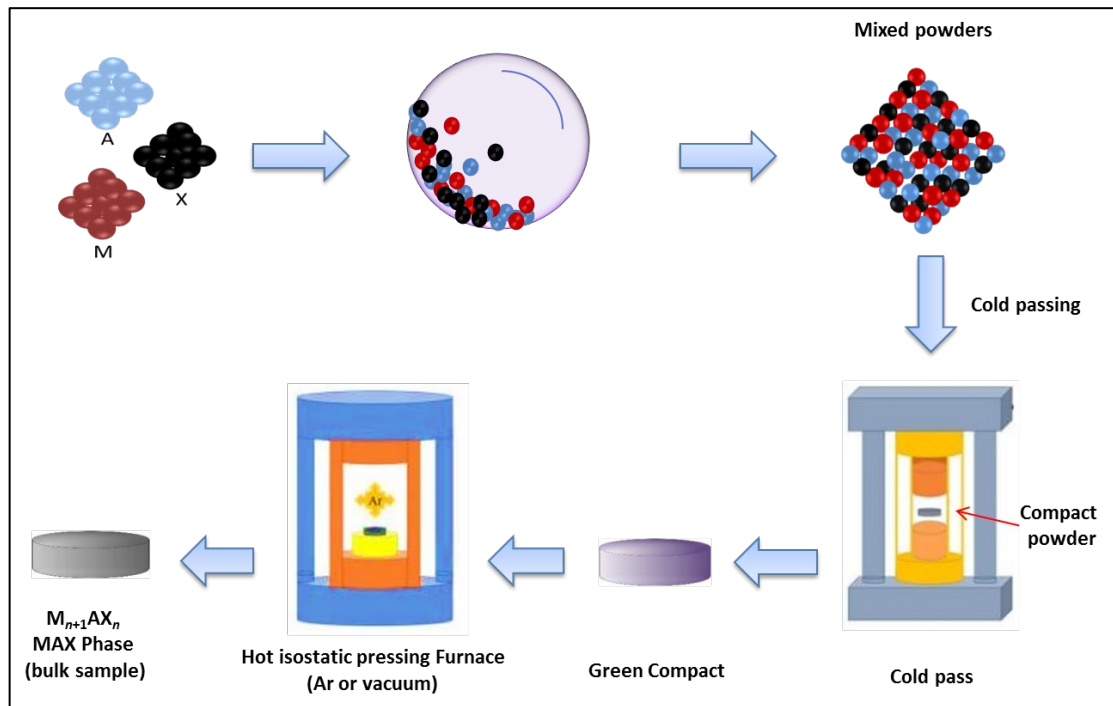
Scheme 1: shows  $M_2AX$  (211) MAX phase structure

**Table 1:** Shows the comparison between synthesis process of the MAX phase [28, 41]

Synthesis methods	Advantage	Disadvantage	Application	Phase purity
Pressureless sintering(PS)	Simple setup High purity product Easy scalable	Higher reactant loss Low density product (70%)	Product MAX phase suitable for grinding to powder	Up to 99% Generally much lower
Hot pressing sintering (HP)	highest quality of Product and high density	Small batch size And high cost equipment	High quality sample and size <100mm	> 99%
Self-propagation sintering (SHP)	Significantly reduce input energy, time and low cost	Lack of control over reaction Low density 50%	Rapid energy efficiency method of producing materials suitable to powder	~ 90%
Hot isostatic pressing sintering (HIP)	successfully synthesize monolithic bulk MAX phases	Small batch size And high cost equipment and control	fabricating high pure bulk MAX phases	> 99%

## 2.1 Synthesis of $Zr_2InC$ MAX Phase

Manoun et al. fabricated  $Zr_2InC$  using Zr, In, and C powders synthesizing bulk polycrystalline samples of  $Zr_2InC$ , which are pre-sintering in vacuum and sealed tubes of glass. These sealed glass tubes were subjected in hot isostatic pressing sintering (HIPS) Scheme 2 at 1300°C for 7 hours under 90 MPa. The HIPS samples were primarily single phase, according to X-ray powder diffraction. The predominant impurities were < 3.5 vol% (In) element, mostly at boundaries of grain with  $ZrC$  < 2 % of volume, according to microstructural studies and differential scanning calorimetry. The dense grain size ranged from 5 to 10  $\mu m$ . The discovered MAX phases are a hexagonal crystal structure. Even under high pressure of 52 GPa, no further peaks can be seen in the XRD spectrum. This structure is therefore stable, similar to the other MAX phases that are investigated recently [42].

**Scheme 2:** Shows The MAX Phase Hot Isostatic Press Sintering

Hoffman et al., synthesized  $Zr_2InC$  MAX phase utilizing ball milling. The main raw materials in this case are Zr, In and graphite. In borosilicate glass tubes, the mixed powders were sealed under vacuum before being heated to 500°C in air for two hours and then for 9 hours in 600 °C. After collapsing, the containers put in a hot isotactic press HIP. The Argon gas pressure was raised to 70 MPa while the HIP was heated to 750°C in 2 hours and held there for 1.5 hours. The temperature was immediately raised to 1300 °C following compression and maintained there for 12 hours with 90 MPa. According to XRD, SEM, and TEM analyses, few volume fractions of non-reacted indium and zirconium carbide were found at the boundaries of grain that is completely dense (single-phase  $Zr_2InC$  samples). According to DSC analysis, the indium content is approximately about 3.6 % vol. The majority of the obtained grains were from 3 to 5  $\mu m$  [43].

Gupta and co-workers synthesized  $Zr_2InC$  using the HIPS technology. They milled the powders using a ball mill (using alumina balls) for 1 hour in a container of plastic to obtain stoichiometric properties. In tubes of borosilicate glass the blended powder was enclosed and heated for 10 hours to temperature of 650°C. The tubes were collapsed and the powder was able to

preheat as a result of the HIP method. They used a hot isostatic press (HIP) to heat the collapsed tubes to 750°C. It was pressed to 70 MPa before being heated for 12 hours to temperature of 1300°C, and the samples were kept at this temperature. Based on the results of this research, it appears that the moderate temperatures in air are the only one method to investigate the ternary carbides. The ternary carbides rapidly oxidizing to form transition metal oxides as well as  $\text{In}_2\text{O}_3$ . Given that oxygen can easily penetrate even the most oxidation-resistant substance,  $\text{M}_2\text{InC}$  phases. These low friction and wear materials can be used for a variety of applications of important technologically fields such as electrical spinning connections, rotating bearings and others [44].

## 2.2 Synthesis of $\text{Zr}_2\text{SnC}$ MAX Phase

For the first time, M. Barsoum et al. tried to offer a processing technique that enabled them to create four known Sn-containing H-phases  $\text{M}_2\text{SnC}$ . They show some preliminary property measurements obtained on these products. This phases are polycrystalline and totally dense with single-phase samples. The bulk polycrystalline sample  $\text{Zr}_2\text{SnC}$  was produced by stoichiometrically combining graphite, tin and transition metal powders (all powders were 325 mesh, 99% purity). The powders were blended for two hours in a V-blender type blender before being cold pressed at 138 MP into a stainless steel die. The Pyrex test tube was used to vacuum-seal green bodies and then placed in a HIPS chamber, and they used a temperature of 1250 °C. They discovered that the formation of this ternary carbide, or MAX phase, is hindered by the fact that their reaction kinetics are slow at low temperatures ( $\approx 1000^\circ\text{C}$ ), but that they decompose at higher temperatures ( $\approx 1350^\circ\text{C}$ ). The uniqueness of this layered compound is that it is easily machinable as graphite and it has excellent electrical conductivity, with a conductivity of about  $7 \times 10^6 (\Omega\cdot\text{m})^{-1}$ . The  $\text{Zr}_2\text{SnC}$  resistivity temperature coefficient is 0.004 1/K and shows a metallic-like temperature dependency of the resistivity. This ternary had a hardness of  $3.5\pm 0.4\text{GPa}$ [45]. Table 2 illustrates properties of synthesized  $\text{Zr}_2\text{SnC}$ .

El-Raghy et al. produced  $\text{Zr}_2\text{SnC}$  samples that were mostly single phase (92–94 vol.%) and fully dense using HIP (Reactive sintering is a type of sintering in which the chemical reaction between the contents of the green compact and its densification happen at the same time [35] at a temperature of 1200°C for 12 h with a HIP pressure increase to 70 MPa. The  $\text{Zr}_2\text{SnC}$  MAX phase is considered to be effective electrical conductors, readily machinable and have temperature coefficients of resistivity of about  $0.0035 \text{ K}^{-1}$ . The resistivity temperature coefficients, Vickers hardness, thermal coefficients of expansion (TCEs), and Young's modulus are shown in the Table 3. They discovered that at the 1250-1390 °C temperature range, the synthesized ternary carbides dissociated to A member of IIIA or IVA group and carbide of transition metal [46].

**Table 2:** shows the  $\text{Zr}_2\text{SnC}$  properties synthesis by Barsoum et al.,[45]

Theoretical density ( $\text{g}/\text{cm}^3$ )	Measured density ( $\text{g}/\text{cm}^3$ )	Dissociated Temperature ( $^\circ\text{C}$ )	Processing Temperature ( $^\circ\text{C}$ )	Conductivity ( $\text{m}\cdot\Omega^{-1}$ )	Resistivity Temperature coeff ( $\text{k}^{-1}$ )	Vickers hardness GPa
7.16	6.98	$1260 \pm 25^\circ\text{C}$	1250	$7 \times 10^6$	0.004	$3.5 \pm 0.4$

**Table 3:** Shows the properties of synthesis  $\text{Zr}_2\text{SnC}$  and  $\text{Zr}_2\text{PbC}$  by El-Raghy et al.,[46]

Sample	Thermal expansion coeff. ( $\text{ppm}/\text{K}$ )	Dissociated Temp ( $^\circ\text{C}$ )	Processing Temp ( $^\circ\text{C}$ )	Conductivity ( $\text{m}\cdot\Omega^{-1}$ )	Resistivity Temp. coeff ( $\text{k}^{-1}$ )	Vickers hardness (GPa)	Elastic modulus (GPa)
$\text{Zr}_2\text{SnC}$	$8.3 \pm 0.2$	1275	1200	$2 \pm 14 \times 10^6$	0.0035	$3.9 \pm 0.3$	178
$\text{Zr}_2\text{PbC}$	$8.2 \pm 0.2$	<1300	1200	$2 \pm 14 \times 10^6$	0.0144	$3.8 \pm 0.7$	_____

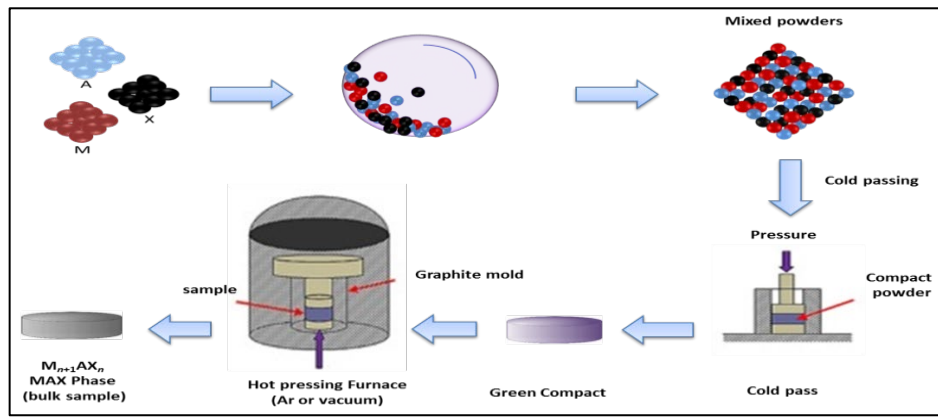
## 2.3 Synthesis of $\text{Zr}_2\text{PbC}$ MAX Phase

For the first time, El-Raghy et al. produced mostly single phase of about 92 to 94 vol.% and  $\text{Zr}_2\text{PbC}$  that totally dense samples by utilizing the HIPS technique at a temperature of 1200 °C for 48–96 hours with a HIP raised to 70 MPa. At room temperature, the ternaries MAX phase  $\text{Zr}_2\text{PbC}$  is unstable in the natural atmosphere. The  $\text{Zr}_2\text{PbC}$  MAX phase is considered as good electrical conductors with resistivity temperature coefficients of about  $(0.0144) \text{ k}^{-1}$  and readily machinable property. The range of vickers hardness values is around  $(3.8 \pm 0.7) \text{ GPa}$ . Pb-containing ternaries had thermal coefficients of expansion (TCEs) that were almost near or equal level with Sn-containing ternaries. Zr-containing ternaries carbides have thermal expansion coefficients of around  $(8.2 \pm 0.2) \times 10^6 \text{ K}^{-1}$  as illustrated in Table 3 [46].

## 2.4 Synthesis of $\text{Zr}_2\text{AlC}$ MAX Phase

Lapauw and coworkers studied synthesis temperature that effect on the structure of the  $\text{Zr}_2\text{AlC}$  MAX phases. They claimed that the hot pressing technique (HP) Scheme 3 can successfully synthesize the ceramic MAX phase of the  $\text{Zr}_2\text{AlC}$  at a temperature rang 1475-1575°C for 0.5 h, with the impure ZrC component as a secondary phase. Upon achieving dwell temperature, 7 MPa initial applied load was increased to 20 MPa. Additionally, Lapauw and coworkers showed that the temperature of the synthesized was about 1525 °C and the yield of  $\text{Zr}_2\text{AlC}$  MAX phase was about 67 wt. % with 33 wt.% of  $\text{ZrC}_x$  as an impurity component. The difficulties are encountered in this research to obtain the  $\text{Zr}_2\text{AlC}$  MAX phase at a low temperature with high purity [39].

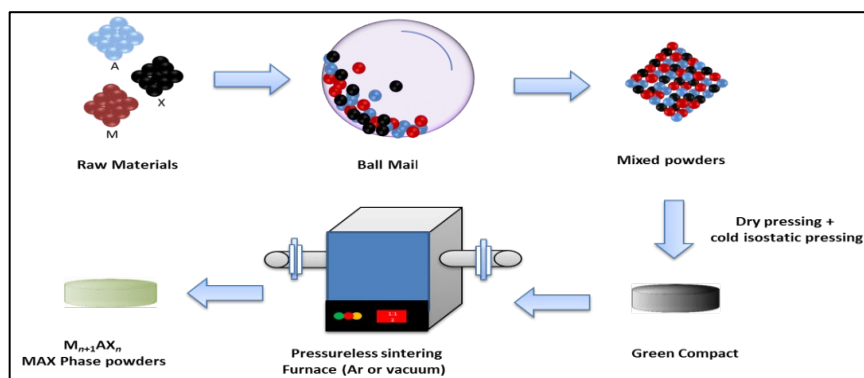




Scheme 3: Shows The MAX Phase Hot Press Sintering

Haemers and colleagues proposed that the ceramic MAX phase  $Zr_2AlC$  may be produced utilizing the hot press (HP) process. They were successful reducing the impure quantities of  $Zr_3AlC_2$  and  $ZrC_x$  components. The sintering temperature ranged from 1525 to 1575 °C for 0.5 h under a pressure increase from 7 MPa to 20 MPa. The mixing ratio is 2Zr: 0.8Al: 1.2C and the heating rate is 25 °C.min<sup>-1</sup>. Using a pressureless sintering (PLS) approach, the researchers attempted to synthesize ceramic  $Zr_2AlC$  MAX phase. The samples were sintered for 10 minutes at 1900 °C before being kept at 1600°C (1 hour), 1450°C (1 hour), 1300°C (1 hour), and 1150°C (10 hours) under an argon gas environment and at a heating range of 20°C /min. The ZrC component formation at high temperatures with Zr-Al alloy components is a significant problem that researchers face with this process. The researchers also assumed that the PLS method is used to combine zirconium with additional substances such as Cr, Mo, or Ti to create  $(Zr_xM_{1-x})_2AlC$  compounds. None of these compounds, however, contains a Zr-based MAX phase. According to this study, pressureless sintering is not be capable producing the  $Zr_2AlC$  MAX phase with high purity [47].

Horlait and co-workers attempted to partially substitute one of the components of  $Zr_2AlC$  in order to stabilize the MAX phase. They provided details to synthesize two types of the quaternary MAX phases. They created  $(Zr, M)_2AlC$  and  $Zr_2(Al, A)C$  quaternary MAX phases, M stands for Cr, Ti, or Mo and A stands for S, As, Sn, Sb, or Pb. For  $ZrH_2$ ,  $ZrC$ ,  $TiH_2$ , As, Cr, Mo, Sn, Pb, Al,  $Al_2S_3$ , Sb and graphite were maintained in jars for milling process. The  $ZrO_2$  balls of 10 mm were used to fill milling jars with argon (Ar). The jars were sealed and spun at 360 rpm for 0.5 hours. In tightly sealed bottles of plastic, the powders were kept after being delivered to the glove box and kept there. They modified the stoichiometry ratio for the  $(Zr + M)$ ,  $(Al + A)$ , and C MAX phases to be 2/1.05/0.95, respectively. The reactions were carried out in graphite crucibles using powders pressureless sintering of the in Argon gas as see in Scheme 4. There were four different synthesis temperatures that can be used such as 1900 °C for 10 min, 1600 °C and 1450 °C for 1 hour, 1300 °C and 1150 °C for 10 hours at rate of heating 20°C min<sup>-1</sup>. No Zr-containing MAX phases were produced in  $Zr_2AlC$  when Zr was partially replaced by Mo, Ti, or Cr. Similar results were not obtained when Al was substituted for as or even S. The Al has been partially replaced, although, heavier MAX formers like tin, Antimony, lead, and bismuth.  $Zr_2(Al_{0.2}Sn_{0.8})C$ ,  $Zr_2(Al_{0.3}Sb_{0.7})C$ ,  $Zr_2(Al_{0.35}Pb_{0.65})C$ , and  $Zr_2(Al_{0.42}Bi_{0.58})C$  are the end products. These compounds contain only trace amounts of Al. This proves that partial replacements on the A-sites can still result in the desired  $Zr_2AlC$  phase [48]. Green compact Tunca et al, produced MAX phases using a technique with conditions of 30 MPa hot pressing and 30 min pressureless sintering for  $(Zr_{1-x}Ti_x)_2(Al_{0.5}Sn_{0.5})C$  MAX phase, x (0 - 1) were at 1450°C in a vacuum environment. The resulting is a double solid solution of MAX phase with virtually pure phase (> 98%). The pressureless sintering ceramics had up to 60% residual porosity while the hot pressed ceramics had a complete densification. This high purity was examined using the XRD, as well as and minor phases such as intermetallic compound  $Al_2Zr$ ,  $Al_3Zr_2$  and  $Ti_2Sn$ ,  $Al_2O_3$  and carbides  $(Zr,Ti)C$ . The key challenges to achieving a good phase purity was the inclusion of tin element to the  $(Zr,Ti)_2AlC$  MAX phase structure. Sn-containing double solid solutions were found to have lower M6A prismatic distortion values than  $(Zr,Ti)_2AlC$  MAX phases. Once the  $(Zr,Ti)_2(Al_{0.5}Sn_{0.5})C$  MAX phases were comparable to the  $Zr_2(Al_{0.5}Sn_{0.5})C$  and  $Ti_2(Al_{0.5}Sn_{0.5})C$  end-members, the anisotropy of thermal expansion was enhanced [40].



Scheme 4: Shows The MAX Phase Pressureless Sintering

Ali et al, study the First principles calculations based on density functional theory (DFT) to examine the impacts of M atomic species mixing on the structural, elastic, electrical, thermodynamic, and charge transport properties of newly synthesized MAX phase  $(Zr_{1-x}Ti_x)_2AlC$  ( $0 \leq x \leq 1$ ) solid solutions. It is discovered that the lattice constants decrease with Ti content, which is in good agreement with the experimental findings. These solid solutions' mechanical stability criteria are satisfied by the elastic constants. Up to  $x = 0.67$ , it is discovered that the constants C11, C33, and C44 rise with Ti concentrations before significantly falling after that. C12 and C13 exhibit a counter-trend. Additionally, it is discovered that the elastic moduli rise up to  $x = 0.67$ , after which they start to significantly decline. The both Pugh's ratio and the Poisson's ratio support the brittleness of  $(Zr_{1-x}Ti_x)_2AlC$ . These solid solutions were anisotropy and likely metallic in nature. The electronic structure has revealed a mixture of covalent, ionic, and metallic bonding, with covalent bonding predominating as a result of the hybridization of Zr-4d states and C-2p states. The calculated Debye temperature and minimum thermal conductivity are found to rise with Ti contents, while the melting temperature is highest for  $x = 0.67$ . In comparison to the two end members,  $Zr_2AlC$  and  $Ti_2AlC$ , the solid solution at  $x = 0.67$  exhibits better mechanical and thermal properties. At 400 K,  $(Zr_{1-x}Ti_x)_2AlC$  has the highest power factor ( $S^2 \sigma/\tau = 11.1 \times 10^{10} \text{ Wm}^{-1}\text{K}^{-2}\text{s}^{-1}$ ) [49].

Ali et al, investigated the First-principles density functional theory (DFT) computations were used to examine the structural, elastic, and electrical properties of newly synthesized  $Zr_2(Al_{0.58}Bi_{0.42})C$ ,  $Zr_2(Al_{0.2}Sn_{0.8})C$ , and  $Zr_2(Al_{0.3}Sb_{0.7})C$  MAX nanolaminates. For these compounds, theoretical Vickers hardness has also been estimated. Where applicable, all the computed results are compared to experimental data as well as data from the recently discovered  $Zr_2AlC$  phase. These two  $Zr_2(Al_{0.58}Bi_{0.42})C$  and  $Zr_2(Al_{0.2}Sn_{0.8})C$  compounds are the first MAX compounds that incorporate Bi and Sn. The estimated structural parameters and the experimental results are found to be in good agreement. The mechanical stabilities of these compounds have been theoretically supported by calculations of the polycrystalline elastic coefficients and various single crystal elastic constants, including  $C_{ij}$ . The partial Bi/Sn/Sb substitution for Al in  $Zr_2AlC$  results in an increase in the bulk modulus and a decrease in the shear modulus. These Bi/Sn/Sb containing MAX phases are more anisotropic than  $Zr_2AlC$ , exhibit a tendency toward ductility and have a lower Vickers hardness. The Zr 4d orbitals contribute mostly to the metallic characteristics of the electronic band structures. Bi, Sn, and Sb atoms can partially raise the EDOS at the Fermi level[50].

## 2.5 Synthesis of $Zr_2SC$ MAX Phase

Opeka et al. synthesized the  $Zr_2SC$  ceramics MAX-phase by mixing process including  $ZrH_2$ , carbon or  $ZrC$ , and  $ZrS_2$ ,  $WS_2$ , or  $FeS_2$  as sulfur sources and hot pressing. The powder combinations were performed in helium with  $ZrS_2$  with the range of temperature about 1300–1650°C from 30 to 90 minutes with 20 MPa. The  $Zr_2SC$  ceramics made from  $FeS_2$ ,  $ZrH_2$ , and  $ZrC$  at 1750°C had a typical MAX-phase layered structure, good thermal shock resistance, thermal stability to 2100°C. Up to 800°C, 250 MPa was the flexural strength, 38  $\text{W} \cdot (\text{m}\cdot\text{K})^{-1}$  at 100 °C to around 30  $\text{W} \cdot (\text{m}\cdot\text{K})^{-1}$  at 1100 °C was thermal conductivity range, and  $(0.4 - 0.5) \text{ kJ} \cdot (\text{kg} \cdot ^\circ\text{C})^{-1}$  at temperatures between 100 and 1100 °C specific heat ranging. In the 25–2000 °C temperature range the coefficient of thermal expansion was  $8.8 \times 10^{-6} (\text{ }^\circ\text{C})^{-1}$ . Load –deflection curves revealed plastic deformation at room temperature to 2066°C. Temperature had a considerable effect on sample deflection at fracture, with a minimum temperature at 1510 °C. The material generated an adhering, protective scale after 23 seconds of arc heater testing at 2150 °C[51].

Tomohige et al. discovered the SHS process that can readily produce  $Zr_2SC$ , with  $ZrC$  and  $Mo_2C$  as byproducts. The basic composition of the MAX phase was established as  $Zr:S:C = 2:1:1$ . In the molar ratio  $Zr_{2-x}Mo_xSC$  ( $x = 0-1.2$ ), the molybdenum transition metal element was added in order to try to form a solid solution of the MAX phase. A metal heating coil was used to establish the SHS process. The MAX phases were synthesized showing an evidence of the formation of solid solution with up to 20% Mo to Zr, according to XRD measurements. The monolithic  $Zr_2SC$  phase interlayers were discovered to be tightly bonded to one another by SEM test, and the structure appeared to be one in which interlayer exfoliation could be challenging. Moreover, the interlayer structure of the molybdenum-added MAX phase is easy to exfoliate. Because the material properties of the Mo-added  $Zr_2SC$  MAX phase differed from those of monolithic  $Zr_2SC$ . It was inferred that the Mo-added one may be a promising material, particularly in terms of solid lubricity. The TEM studies revealed that the Mo-added MAX phase was made up of thin layers with a 10 nm thickness [52].

## 2.6 Synthesis of $Zr_2SeC$ - $Zr_2SC$ MAX Phases

Wang synthesized bulk  $Zr_2SeC$  MAX phase using commercially available powders. For 30 minutes in an argon environment, zirconium diselenide  $ZrSe_2$ , zirconium, and carbon were combined in the following molar ratio: 1.05:3:1.95 In a graphite mold, cold pressing was used to form the powder mixture. Under an argon environment, the  $Zr_2SeC$  mass was in situ sintered using a pulse-electric-current-assisted sintering apparatus. These green pellets were initially heated at a range of 50°C.  $\text{min}^{-1}$  from 450°C to 1100°C, while the temperature range from 1100°C to 1500°C was applied at a range of 25 °C.  $\text{min}^{-1}$ . The pressure (48 MPa) was applied to the pellets as the temperature raised, and the pellets were maintained at the desired temperature for 20 minutes. For the  $Zr_2SeC$  phase, similar details were used. The iron particles were removed from the pellets by further grinding them and submerging in a solution of hydrochloric acid (1 M) at 45°C for two days. In the pulse-electric-current-assisted sintering method, the iron-removed powders were employed to create high density  $Zr_2SC$  monolith. Under an argon environment, the pellets were sintered for 20 minutes at 1600 °C with 48 MPa pressure. They discovered that according to the anisotropy of hexagonal crystals, the thermal expansion of MAX phases in various directions tended to differ from one another. They discovered that according to the anisotropy of hexagonal crystals, the thermal expansion of MAX phases tended to differ in various directions.  $Zr_2SC$  has lower coefficients of thermal expansion (CTEs) than  $Zr_2SeC$  attributed to the strong M-S bond. The CTEs of the Se-MAX phases were interestingly greater than those of the S-MAX phases, indicating that the A elements were necessary for the MAX phase's thermal expansion as well as other physical characteristics. Zr-Se had a bond

length of 2.800, while Zr-S had a bond length of 2.691. The examination of state density in earlier publications also supported the Zr-Se bonding energy being weaker than Zr-S's. As shown by a large thermal expansion in  $Zr_2SeC$ , the amplitude of vibration was enhanced by the flexible crystal structure. They propose that, in accordance with the level of anisotropy proportions for thermal expansion, isotropic expansion increases with temperature [53].

### 3. Future Perspective with Applications of $Zr_2AC$ MAX Phase

The outstanding performance of MAX phase materials, which combine metals and ceramics, can pay a lot of attention. These materials are machinable, electrically and thermally conductive, not prone to thermal shock, plastic at high temperatures, and extremely damage-tolerant. They therefore provide ideal choices for high-temperature technologies, such as components, sliding electrical contacts, contacts for 2D electronic circuits, Li-ion batteries, wear- and corrosion-resistant coatings, superconducting materials, spintronic, and the nuclear sector. Strong covalent M-X bonds and comparatively weak metallic M-A bonds are seen in MAX phases' structures, which contribute to their hybrid properties. Scientists are always motivated by these difficult characteristics, which has led to the recent discovery of more than 150 MAX phases [12]. Nuclear reactor designers are becoming more interested in Zr-based MAX phases because of its exceptional neutronic capabilities. Zr is neutron transparent because its thermal neutron absorption cross-section is relatively tiny (Zr atoms have a small cross section for thermal neutrons), which can help nuclear reactors maintain a high neutron economy. As a result, it is routinely utilized in today's nuclear reactors [54]. Aside from economic reasons, Next-generation (Gen-III+) light water reactors (LWRs) require fuel cladding materials that can survive difficult operating circumstances such high mechanical and thermal loads, large neutron irradiation doses, and intensely oxidizing or corrosive environments[39]. either as coatings or in mass Because of their exceptional characteristics, MAX phases are regarded as potential materials for applications such as fuel cladding [39], [54]. The MAX phase applications of  $Zr_2AC$  is widely explain in the next sections.

#### 3.1 Nuclear Application

The  $Zr_2AlC$  phase is the most attractive among all non-synthesizable ternary MAX phases, particularly for the nuclear industry because Zr possesses outstanding reactor neutronics and fuel economy qualities and a high neutron transparency. Additionally, the presence of the Al component is intended to increase the resistance to high-temperature steam oxidation due to its ability to facilitate the layer of protective oxide creation [55,56]. Since good oxidation resistance at high temperatures is predicted for  $Zr_2AlC$ , which has been established for other Al based MAX phases, it is strongly regarded as a protective material in modified Accident Tolerant Fuel (ATF), assembly grids [48]. The  $Zr_2AlC$  phase has attracted interest as a potential accident fuel (ATF) cladding for third-generation light-water reactors (LWRs) and fourth-generation fission reactors due to its high radiation tolerance, oxidation and corrosion resistance, mechanical characteristics, and chemical stability [37]. Despite being suitable for using as cladding materials in nuclear power reactors, zirconium alloys perform poorly in Loss of Coolant Accidents LOCAs, such as those that happened at Chernobyl in 1986 and Fukushima in 2011. The MAX phases' improved oxidation and corrosion resistance makes them a good choice to coat or replace zirconium alloy claddings. Dense, completely pure, homogeneous, and non-textured coatings made of MAX phases should be created at low temperatures to avoid deterioration and/or alteration to the Zircaloy substrates [57]. Following a loss of coolant (LOCA) event that might potentially exceed commercial Zircaloy clads Following a loss of coolant (LOCA) event that might potentially exceed commercial Zircaloy clads, Among the MAX phases of attention for the high-temperature steam atmosphere in next-generation (Gen-III) light water reactors (LWR<sub>s</sub>) (Gen-III+ LWR<sub>s</sub>) is  $Zr_2AlC$  [39].

Exceptional mechanical stability, radiation tolerance, oxidation and corrosion resistance, and compatibility with Pb alloy coolants are essential properties of some MAX phases [58]. It is necessary to look for alternative materials because the majority of nuclear steel grades are susceptible to embrittlement of liquid metal and attack of heavy liquid metal (HLM) under certain operating conditions [59].

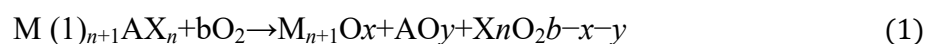
Tunca and Coworkers, claimed that the two promising research directions:

- 1) ZrC-based diffusion barriers on the surface of  $Zr_2AlC$  ceramics may successfully decrease the  $Zr_2AlC$ /lead-bismuth eutectic (LBE) interaction for a long enough time (for example, the lifetime of the substrate fuel clad).
- 2) The in-situ generated  $Zr_2(Al, Bi, Pb)C$  solid solution is a good option for Gen-IV lead-cooled fast reactors (LFR) fuel cladding because it is less neutron-absorbing than  $Zr_2AlC$  and more stable in contact with LBE.

More study is needed to increase the phase purity of ceramics and coatings created from this MAX phase solid solution and to determine the wide range of possible uses [60].

#### 3.2 Oxidation Resistance Application

The following reaction describes how MAX phases typically oxidize at very low temperatures (600°C) [37]:



As a result, the majority of MAX phase are unsuitable for applications of high temperature in environment of oxidizing. additionally , At temperature up to 1400°C, some compositions containing Al as the "A" element can produce an external and adhering  $Al_2O_3$  layer that protects against further internal oxygen diffusion [61]. Unfortunately, not all Al-based MAX phases generate an exterior protective alumina shell due to "competition" between the oxidation of the "M" and "A" elements[62].



### 3.3 Self-Healing of Crack Damage Application

At least three requirements must be met for self-healing behavior to occur, whether it is intrinsic or extrinsic: the agent of healing should be (i) "flow" to the fracture, (ii) fill and closed the volume opened by the crack, and (iii) stick to the surfaces of crack. For  $M_{n+1}AX_n$  phases, oxidation at the fracture surfaces that results in a significant volume expansion takes the role of the "flow" criterion. As a result, it is possible to evaluate the ability of crack healing of MAX phase at high-temperature materials by simultaneously looking at all four of the primary criteria that were proposed: accelerated diffusion of the A-element, volume expansion due to oxidation, adherence of the oxidation product to the matrix, and preferential oxidation of the A-element. The mechanical performance of the filler is also evaluated by comparing the thermal expansion coefficient and Young's modulus of the oxide used to fill cracks with those of the parent material. The latter two criteria are taken into consideration as supporting criteria, creating a total of six considerations to be evaluated for MAX phase compounds that have not yet been looked at for their potential to heal at high temperatures. There four elements arsenic, phosphor, sulfur, and lead that will be eliminated from the 12 A-elements considered for MAX-phases due to the low melting or sublimation points of their oxides. Therefore, the remaining MAX phase compounds that need to be studied only contain Al, Si, Ge, Ga, In, Sn, Tl, or Cd elements. This choice does not include  $M_{n+1}AX_n$  phases with  $n \geq 4$ . The  $Zr_2AlC$  MAX phase is a compound that, through high-temperature selective oxidation, provide the conditions for crack repair [63].

### 3.4 Optical Application

$Zr_2AC$ 's electronic structures revealed that the properties of the metal with covalent bonds are exceptional properties. Excepting the  $Zr_2SC$ ,  $Zr_2AC$  compounds are potential candidates for coatings that can produce the solar heating. The  $Zr_2AC$  MAX phases as an A-group atom traverses through the periodic table from left to right show that the plasma frequency is followed by a decrease in shear stress [64]. The band structure with the absorption and photoconductivity curves, as well as the real and imaginary components of the dielectric constant, all reflect  $Zr_2SeC$  metallic character. Studying the optical characteristics of the  $Zr_2SeC$  has shown its potential for application as a shielding material in order to decrease the heating of solar. The  $Zr_2SeC$  optical characteristics also exhibit anisotropic behavior, similar to its electrical conductivity and mechanical properties [12].

### 3.5 Corrosion Resistance

The potential susceptibility of several MAX phases to environmental-assisted deterioration under both static and fast-flowing exposure conditions (at least 1000 hours at 500°C) was evaluated in an oxygen-poor liquid lead-bismuth eutectic (LBE) environment. There was no indication that LBE had deteriorated despite the constant presence of an external oxide scale. In situ synthesis of  $(Zr,Ti)_{n+1}(Al, pb, Bi)C_n$  solid solutions and partial substitution of Al by Pb/Bi in the crystal structure resulted in the local LBE interaction with the Zr-rich MAX phases. Additionally, the parasitic intermetallic phase was dissolved as a result of the interaction between static liquid LBE and Zr-based MAX phases, enabling LBE to penetrate through to the bulk material. In comparison to 316L stainless steels, the selected MAX phases showed better resistance to dissolution corrosion and erosion [49,50].

### 3.6 MXenes

Naguib et al. discovered MXenes as a novel form of 2-Dimensional material, in 2011. The "A" element is chemically etched to yield the MAX phases, which are then formed through the delamination process. The MXenes have a lot of attention and have been suggested as cathodes for Li and Na batteries, energy storage, water purification and desalination, filtration, sensors, CO catalysts, biosensors, and antibacterial agents due to their high electrical conductivity, hydrophilicity, surface area, and biocompatibility [62]. The MXenes have attracted the attentions of several research organizations and industry, but the only precursors available are the powders of MAX phase. These materials are currently in extremely high demand, which could lead to MAX phase industrial manufacturing [65,66].

### 3.7 Mechanical Application

Yang et al. discovered that  $Zr_2InC$  is an elastic isotropic material with a high degree of anisotropy as pressure increases. As a result, they discovered that the origin of a variety of characteristics is transition from an isotropic to an anisotropic characteristic. The brittleness of  $Zr_2InC$  at ambient parameters was shown by the ratio of the bulk (B) and shear (G) moduli (B/G), as well as B/C44, and the degree of brittleness decreases with pressure [67]. The anisotropic bonding properties of  $Zr_2InC$  and its structural stability make it suitable for usage in future the eventual technological applications [68].

### 3.8 High-Temperature Technology MAX Phase

The previous theoretical and experimental findings led researchers to consider the electrical, bonding, and dynamical characteristics of the  $Zr_2AC$  MAX phase, as well as its mechanical and structural stability, and also its elasticity under pressure. Theoretical analysis of the structural stability, electrical, mechanical, and phonon properties of the  $Zr_2PbC$  MAX phase systems was reported by Alrebdi et al. The results shown that the  $Zr_2PbC$  MAX phases are elastic and electrically anisotropic in nature and appropriate for high temperature applications, optoelectronic devices, and coating materials [69].

A good match for traditional Thermal Barrier Coatings (TBCs) like YSZ ( $10^{-11} 10^{-6} K^{-1}$ ) and the thermally grown oxide (TGO,  $\alpha-Al_2O_3$ ;  $8.5-9.5 10^{-6} K^{-1}$ ) is the Coefficient of Thermal Expansion (CTE) of MAX phases, which is found between non-oxide ceramics and metals in Figure 2. When MAX phases acting as a material for a thermal barrier coating (TBC), For example, MAX phases are utilized because they require some prior knowledge of the Debye temperature, minimum thermal

conductivity, and melting temperature. Ali and colleagues have studied the optical, thermal, mechanical, electrical, and structural characteristics of Zr<sub>2</sub>SeC. The Zr<sub>2</sub>SC MAX phase's characteristics have been compared to those of Zr<sub>2</sub>SeC. They discovered the Zr<sub>2</sub>SeC is soft and has a low value of test of Vickers hardness, such as other MAX phases. Additionally, when compared to a promising TBC material (Y<sub>4</sub>Al<sub>2</sub>O<sub>9</sub>), it is suitable for use in high-temperature technologies, such as thermal barrier coating material TBC. The Zr<sub>2</sub>SeC can also be used as a material for spacecraft covers to lessen solar heating[12]. Table 4 shows the conclusion for MAX phase synthesis methods and its application.

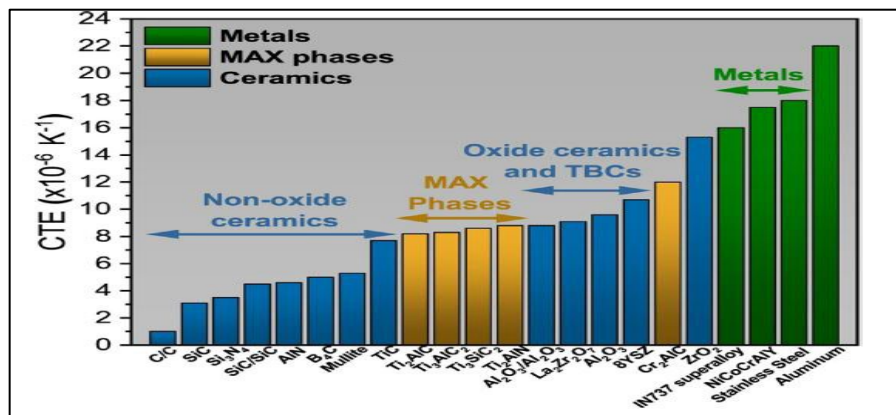


Figure 2: shows the coefficient of thermal expansion (CTE) of typical metals, MAX phases, and ceramics[37]

Table 4: illustration the conclusion of MAX phase synthesis methods and application

MAX Phase	Method	Condition	Purity	Application	Ref.
Zr <sub>2</sub> InC	HIPS	1300°C,7h 90 MPa	—	Oxidation Resistance Self-Healing of Crack Damage	[42]
Zr <sub>2</sub> InC	HIPS	1300°C,12h 70 MPa	—	Mechanical Application MXenes	[43]
Zr <sub>2</sub> InC	HIPS	1300°C,12h 70 MPa	—	MXenes	[44]
Zr <sub>2</sub> SnC	HIPS	1250°C 138 MPa	—	Oxidation Resistance Self-Healing of Crack Damage	[45]
Zr <sub>2</sub> SnC	HIPS	1200°C, 12h 70 MPa	92%- 94%	MXenes	[46]
Zr <sub>2</sub> PbC	HIPS	1200°C 48-96h 70 MPa	92%- 94%	Oxidation Resistance MXenes high-temperature application, optoelectronic devices coating material	[46]
Zr <sub>2</sub> AlC	HPS	1475-1575°C 0.5h 20 MPa	67%	Nuclear Oxidation Resistance	[39]
Zr <sub>2</sub> AlC	HPS	1150-1900°C different time 20 MPa	—	Self-Healing of Crack Damage MXenes	[47]
Zr <sub>2</sub> AlC	PLS	1150-1900°C different time 20 MPa	—	MXenes	[47]
Zr <sub>2</sub> (Al <sub>0.2</sub> Sn <sub>0.8</sub> )C Zr <sub>2</sub> (Al <sub>0.3</sub> Sn <sub>0.7</sub> )C Zr <sub>2</sub> (Al <sub>0.35</sub> Sn <sub>0.65</sub> )C Zr <sub>2</sub> (Al <sub>0.42</sub> Sn <sub>0.58</sub> )C (Zr,Ti) <sub>2</sub> AlC	PLS HP PLS	1150-1900°C different time 20 MPa 1450°C 0.5h 30 MPa	— — — — — > 98%	Oxidation Resistance Oxidation Resistance MXenes	[48]
Zr <sub>2</sub> SC	HP	1750°C 0.5-1.5 h 20 MPa	—	TBCOxidation Resistance MXenes	[51]
Zr <sub>2</sub> SC	SHS	—	20%	—	[52]
Zr <sub>2</sub> SC	HP	1600°C 20 min 48 MPa	—	—	[53]
Zr <sub>2</sub> SeC	HP	1500°C 20 min 48 MPa	—	Oxidation Resistance solar heating coating MXenes	[53]

## 4. Conclusion

The preparation techniques to synthesize  $Zr_2AC$  MAX phases from the essential elements are thoroughly explained in this review. The MAX phases are associated with the extraordinary properties products and their application such solar coatings, oxidation resistance, high temperature applications, and nuclear applications.  $Zr_2InC$  MAX phase is low friction and wear materials can be used for a variety of applications of important technologically such as electrical spinning connections, rotating bearings and others. The  $Zr_2SnC$  MAX phase uses for self-healing of cracks and oxidation resistance. The  $Zr_2PbC$  MAX phases are elastic and electrically anisotropic in nature and appropriate for high temperature applications, optoelectronic devices, and coating materials. Studying the optical characteristics of the  $Zr_2SeC$  has shown its potential for application as a shielding material in order to decrease the heating of solar.  $Zr_2SC$  is suitable for use in high-temperature technologies, such as thermal barrier coating material TBC. The  $Zr_2AlC$  phase is the most attractive among all non-synthesizable ternary MAX phases, particularly for the nuclear industry. The technical methods to synthesize  $Zr_2AC$  MAX phases can be included, Pressureless sintering (PS), Hot pressing sintering (HP), hot isostatic pressing sintering (HIPS) and Self-propagation sintering (SHP). The A concentration of the starting materials, the synthesis temperature, and the holding period must be regulated in order to produce MAX phases with a high degree of purity while taking the vaporization of the A element and the generation of intermediate phases into account. The stability of MAX phases is significantly impacted in some extreme environmental conditions, and thus, the methods of defect formation have a considerable impact on the phases' radiation resistance and self-healing capabilities.

### Authors contributions

All authors contributed to the study conception and design. Material preparation, data collection and analysis were performed by Dumooa R. Hussein, Khalid K. Abbas and Ahmed Al-Ghaban. The first draft of the manuscript was written by Dumooa R. Hussein and all authors commented on previous versions of the manuscript. All authors read and approved the final manuscript.

### Funding

This research received no specific grant from any funding agency in the public, commercial, or not-for-profit sectors.

### Data availability statement

The data that support the findings of this study are available on request from the corresponding author.

### Conflicts of interest

The authors declare that there is no conflict of interest.

### References

- [1] S. G. Vadchenko, D. Y. Kovalev, and M. A. Luginina, Ignition and phase formation in the Zr–Al–C system, *Combust. Explos. Shock Waves*, 53 (2017) 171–175. <https://doi.org/10.1134/S0010508217020071>
- [2] T. A. Alrebdi, M. B. Kanoun, and S. Goumri-Said, Physical properties investigations of ternary-layered carbides  $m_2pb_c$  ( $M = ti, zr$  and  $hf$ ): First-principles calculations, *Cryst.*, 11( 2021) 1445. <https://doi.org/10.3390/cryst11121445>
- [3] A. Azzouz-Rached, M. A. Hadi, H. Rached, T. Hadji, D. Rached, and A. Bouhemadou, Pressure effects on the structural, elastic, magnetic and thermodynamic properties of  $Mn_2AlC$  and  $Mn_2SiC$  MAX phases, *J. Alloys Compd.*, 885( 2021) 160998. <https://doi.org/10.1016/j.jallcom.2021.160998>
- [4] A. Azzouz-Rached, H. Rached, M. H. Babu, T. Hadji, and D. Rached, Prediction of double transition metal ( $Cr_{1-x}Zr_x$ ) $2AlC$  MAX phases as thermal barrier coatings: Insight from density functional theory, *Int. J. Quantum Chem.*, 121(202) 11–13. <https://doi.org/10.1002/qua.26770>
- [5] I. Ouadha, H. Rached, A. Azzouz-Rached, A. Reggad, and D. Rached, Study of the structural, mechanical and thermodynamic properties of the new MAX phase compounds  $(Zr_{1-x}Ti_x)_3AlC_2$ , *Comput. Condensed Matter.*, 23 (2020) e00468. <https://doi.org/10.1016/j.cocom.2020.e00468>
- [6] A. Azzouz-Rached, M. M. Haque Babu, H. Rached, T. Hadji, and D. Rached, Prediction of a new Sn-based MAX phases for nuclear industry applications: DFT calculations, *Mater. Today Comm.*, .27 (2021)102233. <https://doi.org/10.1016/j.mtcomm.2021.102233>
- [7] M. A. Hadi, Superconducting phases in a remarkable class of metallic ceramics, *J. Phys. Chem. Solids.*, 138 (2020)109275. <https://doi.org/10.1016/j.jpcs.2019.109275>
- [8] M. Sokol, V. Natu, S. Kota, and M. W. Barsoum, On the Chemical Diversity of the MAX Phases, *Trends Chem.*, 1 (2019) 210–223. <https://doi.org/10.1016/j.trechm.2019.02.016>

- [9] M. A. Ali and S. H. Naqib, Recently synthesized  $(\text{Ti}_{1-x}\text{Mo}_x)_2\text{AlC}$  ( $0 \leq x \leq 0.20$ ) solid solutions: Deciphering the structural, electronic, mechanical and thermodynamic properties via ab initio simulations, *RSC Adv.*, 10 (2020) 31535–31546. <https://doi.org/10.1039/d0ra06435a>
- [10] A. A. Belkacem, H. Rached, M. Caid, Y. Rached, D. Rached, Nada T. Mahmoud, and N. Benkhetou., The stability analysis and efficiency of the new MAX-phase compounds  $\text{M}_3\text{GaC}_2$  (M: Ti or Zr): A first-principles assessment, *Res.Phys.*, 38 (2022)105621. <https://doi.org/10.1016/j.rinp.2022.105621>
- [11] Y. Rached, A.A. Ait Belkacem, D. Rached, H. Rached, M. Caid, M. Merabet, S. Benalia, L. Djoudi, I.E. Rabah, and M. Rabah, The Stability and Electronic and Thermal Transport Properties of New TI-Based MAX-Phase Compound  $\text{Ta}_2\text{TiX}$  (X: C or N), *Phys. Status Solidi B Basic Res.*, (2022) 2200195. <https://doi.org/10.1002/pssb.202200195>
- [12] M. A. Ali and M. W. Qureshi, Newly synthesized MAX phase  $\text{Zr}_2\text{SeC}$ : DFT insights into physical properties towards possible applications, *RSC Adv.*, 11 (2021) 16892–16905. <https://doi.org/10.1039/d1ra02345d>
- [13] M. A. Ali, M. M. Hossain, M. M. Uddin, A. K. M. A. Islam, D. Jana, and S. H. Naqib, DFT insights into new B-containing 212 MAX phases:  $\text{Hf}_2\text{AB}_2$  (A = In, Sn), *J. Alloys Compd.*, 860 (2021)1–30. <https://doi.org/10.1016/j.jallcom.2020.158408>
- [14] Z. Lin, D. Barbara, P. Taberna, and K. L. Van Aken, Capacitance of  $\text{Ti}_3\text{C}_2\text{T}_x$  MXene in Ionic Liquid Electrolyte. *J. Power Sources*, 326 (2016) 575-579.
- [15] Y. Wang, C. Ma, W. Ma, W. Fan, Y. Sun, H. Yin, X. Shi, X. Liu and Y. Ding, Enhanced low-temperature Li-ion storage in MXene titanium carbide by surface oxygen termination, *2D Mater.*, 6 (2019) 045025. <https://doi.org/10.1088/2053-1583/ab30f9>
- [16] A. M. H. Abdulkadhim, R. Afify, Corrosion Behavior of  $\text{V}_2\text{AlC}$  and  $\text{Cr}_2\text{AlC}$  Materials in Acidic Media., 33 (2015)845–854.
- [17] A. Abdulkadhim, T. Takahashi, D. Music, F. Munnik, and J. M. Schneider, MAX phase formation by intercalation upon annealing of  $\text{TiC}_x/\text{Al}$  ( $0.4 \leq x \leq 1$ ) bilayer thin films, *Acta Mat.*, 59 (2011) 6168–6175. <https://doi.org/10.1016/j.actamat.2011.06.029>
- [18] M. A. N. A., A.A.Atiyah, A. M. H. Abdulkadhim, Investigation of Solid State Reaction in the Ternary Ti-Al-C, Cr-Al-C and V-Al-C Systems A., *Eng.Technol. J.*, 35(2017)764–771.
- [19] S. Aryal, R. Sakidja, M. W. Barsoum, and W. Y. Ching, A genomic approach to the stability, elastic, and electronic properties of the MAX phases, *Phys. Status Solidi (B) Basic Res.*, 251 (2014)1480–1497. <https://doi.org/10.1002/pssb.201451226>
- [20] M. A. Rayhan, M. A. Ali, S. H. Naqib, and A. K. M. A. Islam, First-principles Study of Vickers Hardness and Thermodynamic Properties of  $\text{Ti}_3\text{SnC}_2$  Polymorphs, *J. Sci. Res.*, 7(2015)53–64. <https://doi.org/10.3329/jsr.v7i3.23182>
- [21] M. Griseri, B.Tunca, S.Huang, M.Dahlqvist, J.Rosén, J. Lu, P.O.Persson, L.Popescu, J.Vleugels, K. Lambrinou, Ta-based 413 and 211 MAX phase solid solutions with Hf and Nb, *J. Eur. Ceram. Soc.*, 40(2020) 1829–1838. <https://doi.org/10.1016/j.jeurceramsoc.2019.12.052>
- [22] M. A. Ali, M. S. Ali, and M. M. Uddin, Structural, elastic, electronic and optical properties of metastable MAX phase  $\text{Ti}_5\text{SiC}_4$  compound, *Indian J. Pure Appl. Phys.*, 54 (2016)386–390.
- [23] G. Ying, C.Hu, L. Liu, C. Sun, D.Wen, J. Zhang, Y. Zheng, M.Wang, C. Zhang, X.Wang, C.Wang, Mechanical properties of phase-pure bulk  $\text{Ta}_4\text{AlC}_3$  prepared by spark plasma sintering and subsequent heat treatment, *Process. Appl. Ceram.*, 15 (2021)211–218.
- [24] N. Miao, J. Wang, Y. Gong, J. Wu, H. Niu, S. Wang, K. Li, A.R. Oganov, T. Tada, H. Hosono, Computational prediction of boron-based MAX phases and MXene derivatives, *Chem. Mater.*, 32 (2020)16947–6957. <https://doi.org/10.1021/acs.chemmater.0c02139>
- [25] M. A. Ali, M. M. Hossain, A. K. M. A. Islam, and S. H. Naqib, Recently predicted ternary boride  $\text{Hf}_3\text{PB}_4$ : Insights into the physical properties of this hardest possible boride MAX phase, *J. Alloys Compd.*, 857 (2021) 158264.
- [26] M. W. Qureshi, M. A. Ali, and X. Ma, Screen the thermomechanical and optical properties of the new ductile 314 MAX phase boride  $\text{Zr}_3\text{CdB}_4$ : A DFT insight, *J. Alloys Compd.*, 877 (2021)160248. <https://doi.org/10.1016/j.jallcom.2021.160248>
- [27] Y. CHu, C.C. Lai, Q.Tao, J. Lu, J.Halim, L.Sun, J. Zhang, J.Yang, B.Anasori, J.Wang, Sakka,  $\text{Mo}_2\text{Ga}_2\text{C}$ : a new ternary nanolaminated carbide, *Chem. Commun.*, 51(2015) 6560-6563. <https://doi.org/10.1039/c5cc00980d>
- [28] A.Zhou, 2012. Methods of MAX-phase synthesis and densification–II. In *Advances in science and technology of  $\text{Mn}^{1+}\text{AlX}_n$  phases*, pp. 21-46. Woodhead Publishing.
- [29] M. Radovic and M. W. Barsoum, MAX phases: Bridging the gap between metals and ceramics, *Am. Ceram. Soc. Bull.*, 92 (2013) 20–27.



- [30] H. B. Zhang, Y. C. Zhou, Y. W. Bao, and M. S. Li, Improving the oxidation resistance of Ti<sub>3</sub>SiC<sub>2</sub> by forming a Ti<sub>3</sub>Si<sub>0.9</sub>Al<sub>0.1</sub>C<sub>2</sub> solid solution, *Acta Mater.*, 52 (2004)3631–3637. <https://doi.org/10.1016/j.actamat.2004.04.015>
- [31] F. L. Meng, Y. C. Zhou, and J. Y. Wang, Strengthening of Ti<sub>2</sub>AlC by substituting Ti with V, *Scripta Mater.*, 53 (2005)1369–1372. <https://doi.org/10.1016/j.scriptamat.2005.08.030>
- [32] Y. L. Du, Z. M. Sun, H. Hashimoto, and M. W. Barsoum, Theoretical investigations on the elastic and thermodynamic properties of Ti<sub>2</sub>AlC<sub>0.5</sub>N<sub>0.5</sub> solid solution, *Phys. Lett. A: General, At. Solid State Phys.*, 374 (2009)78–82. <https://doi.org/10.1016/j.physleta.2009.10.023>
- [33] W. Yu, V. Mauchamp, T. Cabioch, D. Magne, L. Gence, L. Piroux, V. Gauthier-Brunet, S. Dubois, Solid solution effects in the Ti<sub>2</sub>Al(C<sub>x</sub>N<sub>y</sub>) MAX phases: Synthesis, microstructure, electronic structure and transport properties, *Acta Mater.*, 80 (2014) 421–434. <https://doi.org/10.1016/j.actamat.2014.07.064>
- [34] Z. Liu, L. Zheng, L. Sun, Y. Qian, J. Wang, and M. Li, (Cr<sub>2/3</sub>Ti<sub>1/3</sub>)<sub>3</sub>AlC<sub>2</sub> and (Cr<sub>5/8</sub>Ti<sub>3/8</sub>)<sub>4</sub>AlC<sub>3</sub>: New MAX-phase compounds in Ti-Cr-Al-C system, *J. Am. Ceram. Soc.*, 97 (2014) 67–69. <https://doi.org/10.1111/jace.12731>
- [35] Z. Liu, E. Wu, J. Wang, Y. Qian, H. Xiang, X. Li, Q. Jin, G. Sun, X. Chen, J. Wang, M. Li, Crystal structure and formation mechanism of (Cr<sub>2/3</sub>Ti<sub>1/3</sub>)<sub>3</sub>AlC<sub>2</sub> MAX phase, *Acta Mater.*, 73 (2014)186–193. <https://doi.org/10.1016/j.actamat.2014.04.006>
- [36] M. W. Barsoum, *MAX phases: Properties of machinable ternary carbides and nitrides*. Wiley, 2013.
- [37] J. Gonzalez-Julian, Processing of MAX phases: From synthesis to applications, *J. Am. Ceram. Soc.*, 104(2021) 659-690. <https://doi.org/10.1111/jace.17544>
- [38] S. T. Ahams, A. Shaari, R. Ahmed, M. C. Idris, N. F. A. Pattah, and U. Teknologi, Ab-initio Calculations of the Structural and Electronic Properties of Zr<sub>2</sub>AlC, *Solid State Commun.*, 1(2020) 41–46.
- [39] T. Lapauw, K. Lambrinou, T. Cabioch, J. Halim, J. Lu, A. Pesach, O. Rivin, O. Ozeri, E.N. Caspi, L. Hultman, P. Eklund, Synthesis of the new MAX phase Zr<sub>2</sub>AlC, *J. Eur. Ceram. Soc.*, 36 (2016)1847–1853. <https://doi.org/10.1016/j.jeurceramsoc.2016.02.044>
- [40] B. Tunca, T. Lapauw, R. Delville, D.R. Neuville, L. Hennet, D.Thiaudière, T.Ouisse, J. Hadermann, J. Vleugels, K. Lambrinou, Synthesis and Characterization of Double Solid Solution (Zr,Ti)<sub>2</sub>(Al,Sn)<sub>2</sub>C MAX Phase Ceramics, *Inorg. Chem.*, 58 (2019) 6669-6683. <https://doi.org/10.1021/acs.inorgchem.9b00065>
- [41] D. T. Cuskelly, *Synthesis of Materials for Energy Applications Focusing on MAX Phases*. PhD diss., University of Newcastle, Australia, 2016.
- [42] B. Manoun, S.K.Saxena, H.P. Liermann, R.P.Gulve, E. Hoffman, M.W.Barsoum, G.Hug, C.S. Zha, Compression of Zr<sub>2</sub>InC to 52 GPa. *Appl. Phys. Lett.*, 85 (2004)1514-1516.
- [43] E. N. Hoffman, M. W. Barsoum, W. Wang, R. D. Doherty, A. Zavaliangos, On the spontaneous growth of soft metallic whiskers, *Proceedings of the Annual Holm Conference on Electrical Contacts*. (2005)121–126. <https://doi.org/10.1109/HOLM.2005.1518232>
- [44] S. Gupta, E. N. Hoffman, and M. W. Barsoum, Synthesis and oxidation of Ti<sub>2</sub>InC, Zr<sub>2</sub>InC, (Ti<sub>0.5</sub>,Zr<sub>0.5</sub>)<sub>2</sub>InC and (Ti<sub>0.5</sub>,Hf<sub>0.5</sub>)<sub>2</sub>InC in air, *J. Alloys Compd.*, 426(2006)168–175. <https://doi.org/10.1016/j.jallcom.2006.02.049>
- [45] M. W. Barsoum, G. Yaroshuk, and S. Tyagi, Fabrication and characterization of M<sub>2</sub>SnC (M = Ti, Zr, Hf and Nb), *Scripta Mater.*, 37 (1997)1583–1591. [https://doi.org/10.1016/S1359-6462\(97\)00288-1](https://doi.org/10.1016/S1359-6462(97)00288-1)
- [46] T. El-Raghy, S. Chakraborty, and M. W. Barsoum, Synthesis and characterization of Hf<sub>2</sub>PbC, Zr<sub>2</sub>PbC and M<sub>2</sub>SnC (M = Ti, Hf, Nb or Zr), *J. Eur. Ceram. Soc.*, 20 (2000)2619–2625. [https://doi.org/10.1016/S0955-2219\(00\)00127-8](https://doi.org/10.1016/S0955-2219(00)00127-8)
- [47] J. Haemers, R. Gusmão, and Z. Sofer, Synthesis Protocols of the Most Common Layered Carbide and Nitride MAX Phases, *Small Methods*, 4 (2020)1–32. <https://doi.org/10.1002/smt.201900780>
- [48] D. Horlait, S. Grasso, A. Chronos, and W. E. Lee, Attempts to synthesise quaternary MAX phases (Zr,m)<sub>2</sub>AlC and Zr<sub>2</sub>(Al,A)<sub>2</sub>C as a way to approach Zr<sub>2</sub>AlC, *Mater. Res. Lett.*, 4 (2016)137–144. <https://doi.org/10.1080/21663831.2016.1143053>
- [49] M. A. Ali, M.M. Hossain, M.A.Hossain, M.T.Nasir, M.M. Uddin, M.Z. Hasan, A.K.M.A.Islam, S.H. Naqib, Recently synthesized (Zr<sub>1-x</sub>Ti<sub>x</sub>)<sub>2</sub>AlC (0 ≤ x ≤ 1) solid solutions: Theoretical study of the effects of M mixing on physical properties, *J. Alloys Compd.*, 743 (2018) 146-154. <https://doi.org/10.1016/j.jallcom.2018.01.396>
- [50] M. A. Ali, M. M. Hossain, N. Jahan, A. K. M. A. Islam, and S. H. Naqib, Newly synthesized Zr<sub>2</sub>AlC, Zr<sub>2</sub>(Al<sub>0.58</sub>Bi<sub>0.42</sub>)C, Zr<sub>2</sub>(Al<sub>0.2</sub>Sn<sub>0.8</sub>)C, and Zr<sub>2</sub>(Al<sub>0.3</sub>Sb<sub>0.7</sub>)C MAX phases: A DFT based first-principles study, *Comput. Mater. Sci.*, 131 (2017)139–145. <https://doi.org/10.1016/j.commatsci.2017.01.048>
- [51] M. Opeka, J. Zaykoski, I. Talmy, and S. Causey, Synthesis and characterization of Zr<sub>2</sub>SC ceramics, *Mater. Sci. Eng., A*. 528 (2011)1994–2001. <https://doi.org/10.1016/j.msea.2010.10.084>

- [52] R. Tomoshige, K. Ishida, and H. Inokawa, Effect of Added Molybdenum on Material Properties of Zr<sub>2</sub>SC MAX Phase Produced by Self-Propagating High Temperature Synthesis, *Mater. Res. Proc.*, 13 (2019) 79–84. <https://doi.org/10.21741/9781644900338-14>
- [53] X. Wang, K. Chen, E. Wu, Y. Zhang, H. Ding, N. Qiu, Y. Song, S. Du, Z. Chai, Q. Huang, Synthesis and thermal expansion of chalcogenide MAX phase Hf<sub>2</sub>SeC, *J. Eur. Ceram. Soc.*, 42 (2022) 2084–2088. <https://doi.org/10.1016/j.jeurceramsoc.2021.12.062>
- [54] H. H. Qarra, K. M. Knowles, M. E. Vickers, S. Akhmadaliev, and K. Lambrinou, Heavy ion irradiation damage in Zr<sub>2</sub>AlC MAX phase, *J. Nucl. Mater.*, 523 (2019) 1–9. <https://doi.org/10.1016/j.jnucmat.2019.05.034>
- [55] J. Fu, T. F. Zhang, Q. Xia, S. H. Lim, Z. Wan, T. W. Lee, K. H. Kim, Oxidation and corrosion behavior of nanolaminated MAX-phase Ti<sub>4</sub>C film synthesized by high-power impulse magnetron sputtering and annealing, *J. Nanomater.*, (2015). <https://doi.org/10.1155/2015/213128>
- [56] D. Horlait, S. C. Middleburgh, A. Chroneos, and W. E. Lee, Synthesis and DFT investigation of new bismuth-containing MAX phases, *Sci. Rep.*, 6 (2016) 1–9. 2016. <https://doi.org/10.1038/srep18829>
- [57] K. L. Murty and I. Charit, Structural materials for Gen-IV nuclear reactors: Challenges and opportunities, *J. Nucl. Mater.*, 383 (2008) 189–195. <https://doi.org/10.1016/j.jnucmat.2008.08.044>
- [58] T. Lapauw, B. Tunca, J. Joris, A. Jianu, R. Fetzer, A. Weisenburger, J. Vleugels, K. Lambrinou, Interaction of Mn+1AX<sub>n</sub> phases with oxygen-poor, static and fast-flowing liquid lead-bismuth eutectic, *J. Nucl. Mater.*, 520 (2019) <https://doi.org/10.1016/j.jnucmat.2019.04.010>
- [59] J. Van den Bosch, R. W. Bosch, D. Sapundjiev, and A. Almazouzi, Liquid metal embrittlement susceptibility of ferritic-martensitic steel in liquid lead alloys, *J. Nucl. Mater.*, 376(2008)322–329. <https://doi.org/10.1016/j.jnucmat.2008.02.008>
- [60] B. Tunca, T. Lapauw, C. Callaert, J. Hadermann, and R. Delville, Compatibility of Zr<sub>2</sub>AlC MAX phase-based ceramics with oxygen-poor, static liquid lead-bismuth eutectic, *Corros. Sci.*, 171 (2020) 108704.
- [61] J. L. Smialek, Oxidation of Al<sub>2</sub>O<sub>3</sub> scale-forming MAX phases in turbine environments. *Metall. Mater. Trans. A*, 49 (2018) 782–792. <https://doi.org/10.1007/s11661-017-4346-9>
- [62] D. J. Tallman, B. Anasori, and M. W. Barsoum, A critical review of the oxidation of Ti<sub>2</sub>AlC, Ti<sub>3</sub>AlC<sub>2</sub> and Cr<sub>2</sub>AlC in Air, *Mater. Res. Lett.*, 1 (2013) 115–125. <https://doi.org/10.1080/21663831.2013.806364>
- [63] A. S. Farle, C. Kwakernaak, S. van der Zwaag, and W. G. Sloof, A conceptual study into the potential of Mn+1AX<sub>n</sub>-phase ceramics for self-healing of crack damage, *J. Am. Ceram. Soc.*, 35 (2015)37–45. <https://doi.org/10.1016/j.jeurceramsoc.2014.08.046>
- [64] A. K. M. A. Islam, Remarkable class of materials: Band structures and optical properties of non-superconducting and superconducting MAX phases, *J. Phys.: Conf. Ser.*, 1718, 2021,012002. <https://doi.org/10.1088/1742-6596/1718/1/012002>
- [65] B. Anasori & Ü. G. Gogotsi. 2D metal carbides and nitrides (MXenes), Berlin: Springer, 2019.
- [66] M. Naguib, V. N. Mochalin, M. W. Barsoum, and Y. Gogotsi, 25th anniversary article: MXenes: A new family of two-dimensional materials, *Adv. Mater.*, 26 (2014)992–1005. <https://doi.org/10.1002/adma.201304138>
- [67] Z. J. Yang, L. Tang, A. M. Guo, X. L. Cheng, Z. H. Zhu, and X. D. Yang, Origin of c-axis ultraincompressibility of Zr<sub>2</sub>InC above 70 GPa via first-principles, *J. Appl. Phys.*, 114(2013)1–11. <https://doi.org/10.1063/1.4819174>
- [68] A. Bouhemadou, Calculated structural and elastic properties of M<sub>2</sub>InC (M= Sc, Ti, V, Zr, Nb, Hf, Ta). *Mod. Phys. Lett.*, B.22 (2008) 2063-2076. <https://doi.org/10.1142/S0217984908016807>
- [69] T. A. Alrebdi, M. B. Kanoun, and S. Goumri-Said, Physical properties investigations of ternary-layered carbides m<sub>2</sub>pb<sub>c</sub> (M = ti, zr and hf): First-principles calculations, *Cryst.*, 11 (2021) 2063-2076. <https://doi.org/10.3390/cryst11121445>